Model Predictive Control for EV chargers coupling electro-thermal and degradation battery models

Xabier Dorronsoro
Faculty of Engineering
Mondragon Unibertsitatea
Mondragon, Spain
xdorronsoro@mondragon.edu

Ricardo De Castro
Department of Mechanical Engineering
University of California, Merced
Merced, CA, USA
rpintodecastro@ucmerced.edu

Jorge Varela Barreras
Department of Electronic Engineering
Univesitat Politècnica de Catalunya
Vilanova i la Geltrú
jorge.varela@upc.edu

Erik Garayalde
Faculty of Engineering
Mondragon Unibertsitatea
Mondragon, Spain
egarayalde@mondragon.edu

Unai Iraola
Faculty of Engineering
Mondragon Unibertsitatea
Mondragon, Spain
uiraola@mondragon.edu

Abstract—This paper presents an energy management algorithm for an Electric Vehicle (EV) charging station equipped with solar energy generation and local battery-based storage. For this purpose, a practical electric, thermal, and aging model of a lithium-ion battery cell is developed. We then leverage this model to develop a Nonlinear Model Predictive Control (NL-MPC) to manage the energy flow between the battery, grid, solar generation and the EV charging loads. The NL-MPC aims to reduce the total operating electricity and battery depreciation costs, while taking into account temperature, state of charge, current and voltage constraints. Simulation results, based on a case study from a Spanish EV charging station, demonstrate the effectiveness of the proposed approach.

Index Terms—Electric vehicle, charging station, MPC, batteries, cost opmitization.

I. Introduction

THE transition from fossil fuel-based vehicles towards EVs with the aim of reducing Green House Gas (GHG) emissions is currently a top priority in most of the world's leading countries [1]–[3]. For example, both California and European Union recently established the goal of selling only EVs within the next decade and completely eliminate local emissions from light-duty EVs. Battery-based EVs are seen as the most promised approach to achieve these goals. It is expected that by the end of 2030 there will be around 30 million zero-emission cars in operation on European roads, many of them equipped with rechargeable batteries [4]. Nevertheless, there are still a number of determining factors that slow down their adoption such as EVs autonomy, battery aging & end of life uncertainty, state of safety and BESS recharging infrastructure & time [5].

This increase in EV adoption will also pose challenges to the grid. Today's grids have not been sized to host large volumes of intermittent distributed generation/consumption scenarios, such as the uncontrolled EV charging demand [6]. Uncoordinated and uncontrolled EV charging might deteriorate the power distribution network performance and could lead to the collapse of existing power grid operation. In the face of these challenges, the emphasis of this research is to introduce new solutions based on BESS to promote new EV charging stations improving the existing infrastructure.

According to the literature, adding local renewable energy generation and storage system, is an effective solution to overcome these load mismatch problems [7]. PV integration has been widely studied mainly for self-consumption-oriented buildings, but in the last years they have started to integrate solar panels into the EV charging facilities, thus achieving technical, economical and environmental improvements [8]–[10]. With only a few exceptions [11], [12], most of the works that are focused on this research do not apply advanced nonlinear cell models for the optimization of the system due to their complexity.

When it comes to optimization, it is also important to take into economic costs. Every component is subjected to an economic cost determined by its manufacturing process and market demand. This rule also applies to batteries, where their manufacturing, assembly, and installation process impact the final cost that the user has to take over. However, most of the control algorithms focus on limiting aging without any variable cost update concerning the other elements involved in the system. Thus, it is assumed that this will optimize the performance of the system.

The objective of this research is to apply semi-empirical and nonlinear electrical, thermal, and aging cell models in order to present an advanced control system for a battery pack located in an EV charging station together with renewable generation systems. This control strategy is based on a nonlinear Model Predictive Control (NL-MPC) with the capability to take full advantage of any forecasted data available for the system. By data, it refers to information such as power profiles, for both generation

and consumption and the anticipated price of energy from the grid (buy/sell).

This work offers two main contributions:

- The first is related to the simplification of the semi-empirical cell model developed in [13]. The original model is too complex to be integrated into optimization-based approaches. In this work, a set of practical model simplifications are developed, which reduces numerical complexity and facilitates integration into optimization-based strategies.
- The second contribution is related to the energy management of the EV charging station with renewable energy sources and local battery-based energy storage. We first develop a real-world case study based on data from a Spanish EV charging station; and then apply a NL-MPC approach to reduce the economic costs and the maximum power peak requirements of the charging station, while taking into account battery aging and enforcing numerous operational constraints.

The paper is organized as follows: Section II introduces the case study, while Section III explains the battery model considered for this work. Then, Section IV briefly presents the chosen nonlinear MPC strategy. Afterward, Section V shows the results obtained, and, finally, Section VI presents the conclusions and future lines.

II. Summary of the Case Study

The case study tackled in this work revolves around a small EV charging station. The station contains four DC fast chargers supplied not only from the grid but also from a local PV system and on-site BESS. This scenario is representative of the EV charging infrastructure that is becoming increasingly available in Spain [14]. An overview of the complete ecosystem is presented in Fig. 1. The main characteristics of the energy generation (PV) and storage (battery) are shown in Table I.

From a power flow perspective, the grid power (P_{grid}), battery power (P_{Bat}) and PV power (P_{PV}) need to match the load requested by the four DC fast chargers (P_{Load}):

$$\begin{aligned} 0 &= P_{PV} + P_{Bat}(SoC, T, i) + P_{Grid} - P_{Load} \\ &= f_P(P_{Load}, P_{PV}, P_{Grid}, SoC, T, i) \end{aligned} \tag{1}$$

The average load profile of the EV charging station P_{Load} and solar energy generation $P_{PV}$are obtained from official data resources in Spain, such as [15] and [16] (see Fig. 1).

We assume the existence of a power converter, which allows us to regulate the energy transferred to/from the battery. The battery pack is composed of N_s is battery cell connected in series and N_p in parallel. All cells are assumed to have identical characteristics. The overall power provided by the battery pack is given by:

$$P_{Bat}(v_{cell}, i) = f_{Bat} = (v_{cell}(SoC, T, i)N_s)(N_p i) \tag{2}$$

where i is the battery current, v_{cell} the average cell voltage, SoC the state of charge and T the battery temperature.

TABLE I
Parameters of the battery pack model.

Variable	Value	Variable	Value
Cell model	US26650FTC1	Cell capacity	3 Ah
Initial cell SoH	1	EoL cell SoH	0.6
Ich maximum	2.85	Idch minimum	20 A
Nominal voltage	3.2 V	BESS power	655 kW
BESS energy	98.3 kWh	BESS cost	34.4 k€
PV power	30 kW	Charger power	44 kW
EV chargers	4	Charger eff	95%
Daily vehicles	20	EV distance	150 km

Our goal is to find the battery current i during the operation of the EV charging station that i) minimizes the grid electricity costs (J_{grid}) and the depreciation costs related to the BESS ownership ($J_{Q_{Loss,\$}}$); ii) while taking into account operational constraints (e.g. temperature and SoC limits) and battery aging factors.

III. Battery Modelling

This section provides the electrical-thermal-aging model of the battery cells. The cell model is based on an semi-empirical characterization of the commercial cell US26650FTC1 which has been previously studied in [13], [17]. This section describes practical simplifications that were performed in order to reduce numerical complexity of the battery prediction model employed in the MPC.

A. Electrical model

The electrical cell model is based on an open circuit voltage (OCV) source (v_{ocv}) in series with a resistor (R):

$$v_{cell}(SoC, T, i) = v_{ocv}\,(SoC) + R\,(T, i)\,i \tag{3}$$

To prevent damage to the battery cell it is necessary to limit the terminal voltage:

$$\underline{v_{cell}} \leq v_{cell} \leq \overline{v_{cell}} \begin{cases} \overline{v_{cell}} = 3.6\text{V} \\ \underline{v_{cell}} = 2.5\text{V} \end{cases} \tag{4}$$

where $\overline{v_{cell}}$ and $\underline{v_{cell}}$ are voltage limits.

1) To simplify the model, the hysteresis effects in the OCV v_{ocv} are neglected; our OCV voltage model is based on the average OCV obtained computed from the charge and discharge of the cell. At the same time, the effect of temperature on the OCV is not significant and therefore is also neglected in this work. Fig.2a compares the experimental OCV data [13], [17] with the linear OCV model adopted in this work. One can observe that the fitting error is very small when the SoC range is limited to range 10% to 90%.
2) The equivalent series resistance (R) plays a key role in predicting the terminal voltage and temperature of the battery. As discussed in [17], this parameter varies with SoC, temperature and current direction (charge/discharge). This multi-factor dependence results in more complex models, which can negatively

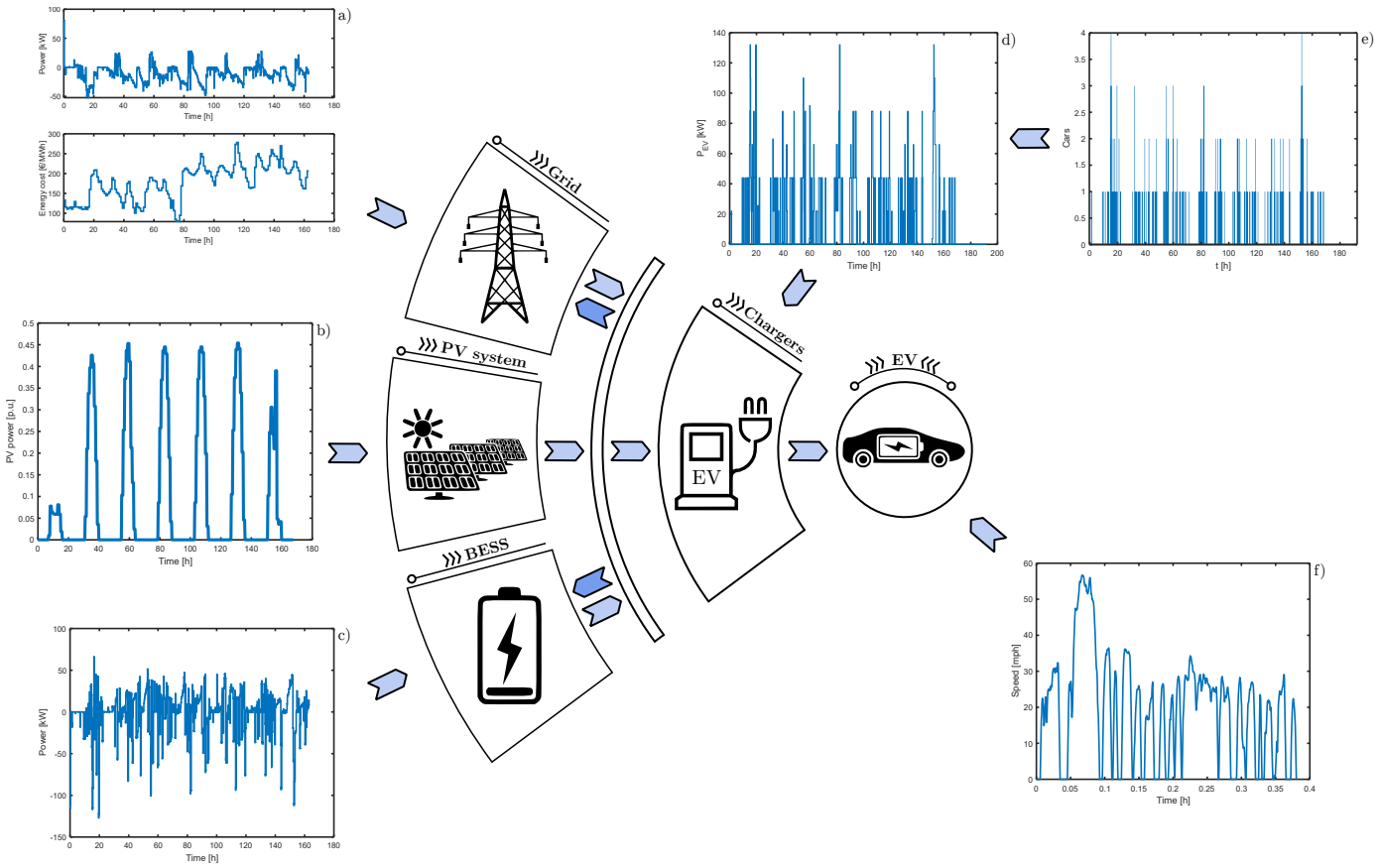

Fig. 1. EV charging station power flow a) grid power and cost, b) solar power generation, c) battery power profile, d) EV charger power profile, e) EV charging station traffic and f) EV battery usage example.

affect the real-time application of optimisation-based techniques in systems with limited computational power. Therefore, we adopted the following simplifications:

- SoC dependence: for each temperature, an average R_{elec} value is estimated based on the values within the operative SoC range (10% to 90%).
- Temperature dependence is captured through the combination of exponential curves(one for charging, the other for discharge):

$$R(T,i) = \begin{cases} a_{ch}e^{b_{ch}T} + c_{ch}e^{d_{ch}T}, & i \geq 0; \\ a_{dch}e^{b_{dch}T} + c_{dch}e^{d_{dch}T}, & i < 0 \end{cases} \quad (5)$$

where $a_{ch}, b_{ch}, c_{ch}, d_{ch}, a_{dch}, b_{dch}, c_{dch}, d_{dch}$ are coefficients defined in Table IV.

B. Thermal model

For temperature prediction (T), a single cell 0D lumped thermal model is considered:

$$\dot{T} = f_T(T,i) = \frac{1}{C_{th}}\left[h_t\left(T_{env} - T\right) + R_j(T,i)i^2\right] \quad (6)$$

where T_{env} is the environmental temperature. The parameters of the model include: i) cell heat capacity (C_{th}), which is computed assuming a cell mass of 85 g and specific heat of 838 J/(kg K) from [17]; ii) the heat transfer between the cell and the ambient (h_t) is established at 0.096 W/K. The temperature bounds for the battery operation are set as:

$$\underline{T} \leq T \leq \overline{T} \begin{cases} \overline{T} = 60°\text{C} \\ \underline{T} = -30°\text{C} \end{cases} \quad (7)$$

C. Aging model

The state of charge (SoC) model captures the normalised amount of energy available in battery:

$$\dot{SoC} = f_{SoC}(i,Q) = \frac{\dot{q}}{Q} = \frac{i}{Q} \quad (8)$$

where Q is the nominal capacity [Ah]. To prevent damage to the battery, the SoC needs to be limited to the range:

$$\underline{SoC} \leq SoC \leq \overline{SoC} \begin{cases} \overline{SoC} = 90\% \\ \underline{SoC} = 10\% \end{cases} \quad (9)$$

The capacity Q decreases over time with the aging of the battery. To account for this battery degradation, we adopt the the semi-empirical model proposed by [13]. The capacity loss in this model is characterized by two main phenomena:

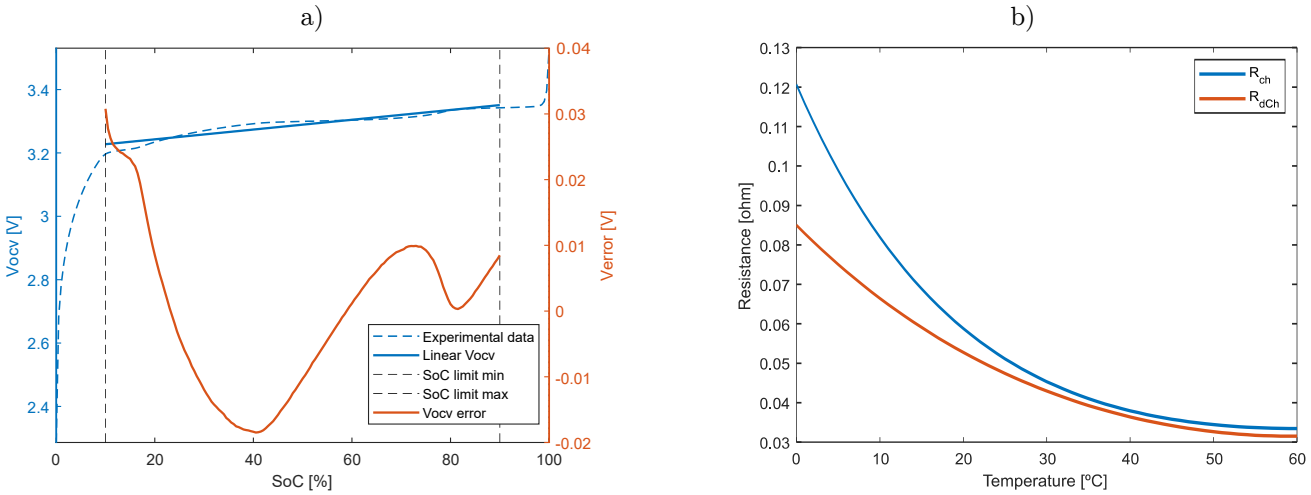

Fig. 2. Electrical parameters of the battery a) Cell's OCV data; b) Ch/Dch electrical resistance model simplification.

- Calendar aging: represents the capacity decrease due to an increase of the solid electrolyte interphase (SEI) at the anode over the life of the battery while there is not any current flow. The degradation is modeled as a temperature and SoC dependent phenomenon ($kCal(T, SOC)$).
- Cycling aging: refers to capacity loss owing to the charge and discharge processes of the cells. This process is highly nonlinear and dependent on the low/high temperature modes. Instead of including the traditional solution of adding Depth of Discharge (DoD) and cycle number dependence, this model works based on the charge throughput.

All these phenomena are briefly presented in the (10) where aging mechanisms can be evaluated through superposition. Each of the integrals represents different capacity loss dependencies to access the full information required for the implementation of the aging aware control strategies:

$$\begin{aligned} Q_{Loss} = & \int k_{\mathrm{Cal}}(T, SOC) \cdot \left(2\tau^{0.5}\right)^{-1} d\tau \\ & + \int k_{\mathrm{Cyc,HiqhT}}(T) \cdot \left(2\varphi^{0.5}\right)^{-1} d\varphi_{\mathrm{Tot}} \\ & + \int k_{\mathrm{Cyc,LowT}}\left(T, I_{\mathrm{Ch}}\right) \cdot \left(2\varphi^{0.5}\right)^{-1} d\varphi_{\mathrm{Ch}} \\ & + \int k_{\mathrm{Cyc,LowT}} \mathrm{H}_{\mathrm{High}}\, \mathrm{soC}\left(T, I_{\mathrm{Ch}}, SOC\right) d\varphi_{\mathrm{Ch}} \end{aligned} \tag{10}$$

where the variables k_{Cal}, $k_{Cyc,HighT}$, $k_{CycLowT}$ and $k_{LowTHighSoC}$ are the stress factors that represent the dependency of each degradation phenomenon due to the different operating parameters such as current, temperature or SoC. Regarding the rest of the parameters, τ represents calendar aging dependence over time and φ refers to charge throughput, being φ_{Ch} the one corresponding only to the battery charging case and φ_{Tot} to the total charge considering both charge and discharge. See [13] for more details.

IV. Nonlinear MPC

This section presents the formulation of the NL-MPC that is used to manage the energy flow in the EV Charging station.

A. Cost Functions

The control goal is to minimize two costs. The first is related to the electricity cost:

$$J_{grid,\$} = C_{grid} \int P_{grid} \quad d\tau \tag{11}$$

where C_{grid} is the cost of energy per kWh in Spain [18]. The second cost captures depreciation costs linked with the battery ownership. To this end, it is necessary to assign an economic value to the maximum useful capacity of the battery until the end of its life. As a first step, it has been determined to establish a linear relationship to determine the cost of the aging rate. This aging rate cost (C_Q) is represented by eq. 12, where Q_{EoL} equals the 60% of the initial capacity and $\$_{bat}$ is the price of 350 €/kWh (assuming product & maintenance cost) of the battery-pack [19].

$$Cost_{cell} = \frac{\$_{cell} Q_{bat} V_{bat}}{Q_{init} - Q_{EoL}} [€/Ah] \tag{12}$$

$$J_{Q_{Loss,€}} = Q_{Loss} Cost_{cell} \tag{13}$$

B. Optimization Problem

The MPC goal is to compute the battery current $u(t) = i(t)$ in order to minimize electricity and battery depreciation costs. To that end, the model introduced in Section III is used to predict the battery response. We first convert this continuous-time model into discrete-time using Euler discretization with sample time t_s. Next, we

combine the cost functions, discretized prediction model and operation constraints to formulate the following MPC problem:

$$\min_{u[k]} J_{mBESS} = \sum_{k=1}^{N} (1-\gamma) J_{Q_{Loss,\$}}[k] + \gamma J_{grid,\$}[k] \quad (14)$$

subject to:

$$\begin{aligned} & SoC[k+1] = f_{SoC}(u[k], Q[z]) \\ & T[k+1] = f_T(T_{env}[k], T[k], SoC[k], u[k]) \\ & 0 = f_P(P_{PV}[k], P_{Load}[k], P_{grid}[k], v_{cell}[k], u[k]) \\ & \underline{SoC} \leq SoC[k] \leq \overline{SoC}, \quad \underline{T} \leq T[k] \leq \overline{T} \\ & \underline{v_{cell}} \leq v_{cell}[k] \leq \overline{v_{cell}}, \quad \underline{u} \leq u[k] \leq \overline{u} \\ & SoC(0) = SoC_0, T[0] = T_0 \\ & k = 0, ..., N-1 \end{aligned} \quad (15)$$

where k in the discrete-time index, and N the prediction horizon.

The objective function $J_{m,BESS}$ is composed of a linear combination between grid and aging costs; The parameter $\gamma \in [0, 1]$ allows the designer to obtain trade-offs between the two costs. The first two constraints are related to the discretized SoC and temperature dynamics. The third constrain enforces the power balance between the PV, battery, grid and the load requested by the DC chargers. The last set of constraints enforces the SoC, Temperature, voltage and current limits, as well as the initial conditions for the battery states (SoC_0, T_0).

The nonlinearities in the prediction model are mainly due to the dependency of the battery model in multiple factors, e.g., the aging costs $J_{Q_{Loss,\$}}$ takes into consideration four different parameters (SoC, temperature, current, and time) in a totally nonlinear function (eq. 10). Note also that the capacity $Q[z]$ needs to be be periodically updated to reflect the battery degradation. We assume that this update occurs at slower time-scale (with time-index z).

The NL-MPC implementation follows a receding horizon strategy, i.e., at every new time step the optimal control action is calculated. Then, the first optimized action $u[0]$ is applied to the BESS. Because of the nonlinear models and the set of hard constraints, finding optimal performance is a challenging task. To assist in the search for optimal solutions, we code the optimization problem in the YALMIP framework [20] an solve it using an interior point optimizer (IPOPT) [21] . Table II provides a summary of the solver parameters employed in this work.

V. Validation Results

This section presents the validation of the NL-MPC framework described in the previous section. To better understand the potential advantages of local storage and optimization-based control, we consider three scenarios:

- Scenario 1 (E1): the EV charging station is only supplied with energy from the grid. No local energy storage is considered.

TABLE II
IPOPT optimizer parameters.

Parameters	Value
Prediction horizon (N)	20
Weight factor: battery	0.2
Weight factor: grid (γ)	0.8
Optimization step time (t_s)	15 min
Simulation step time	3 min
Optimization solver	IPOPT
Initial guess	Yes
Maximum iterations	5000
Maximum CPU time	60 secs
Optimization tolerance	5e-6

- Scenario 2 (E2): the PV system is used as a power supply to reduce the energy consumption of the grid. Season variation is taken into consideration distinguishing between winter ($E2_w$) and summer ($E2_s$) periods.
- Scenario 3 (E3): a BESS is used together with PV system and the grid to supply the EV charging station demand. For the management of this complex system the NL-MPC enables the data acquisition about solar radiation, temperature, and traffic at the charging station in order to provide the best solution. Different seasons are taken into account (winter: $E3_w$; summer: $E3_s$).

Fig. 3 and Tab. III present the obtained results. All the results are based on a one week of EV charger usage; the average environment temperature values are ≈5ºC for winter and ≈25ºC for summer. On average, the numerical interior-point solver required 7s to solve the MPC optimization problem on a regular desktop PC. This is significantly inferior to the controller sample time (15 minutes).

When looking at the power profiles operated by the grid, the use of a BESS with an NL-MPC that forecasts traffic reduces the peak power demand to 53.47 kW in winter, while in summer is 49.83 kW. If we bear in mind that the maximum power peak in the other scenarios is around 132 kW, a reduction of up to 62.3% is achieved. Furthermore, from the distribution network point of view, the operation profile in $E3_w$ and $E3_s$ present less aggressive oscillations than in all other scenarios, crucial for the reliability of the grid.

To analyze the aging of the battery system, even if calendar aging is a relevant capacity loss source, in $E3_w$ and $E3_s$, temperature-related cycling degradation phenomena are dominant (simulations under worst temperature conditions). Accordingly, both low-temperature degradation during winter and high-temperature aging during summer are the factors that cause 46.3% and 46.6% of the total capacity loss.

When it comes to the economic benefits of the system, the results show that adding PV (E2) decreases the overall grid costs (see Table III) by 8% during the winter and

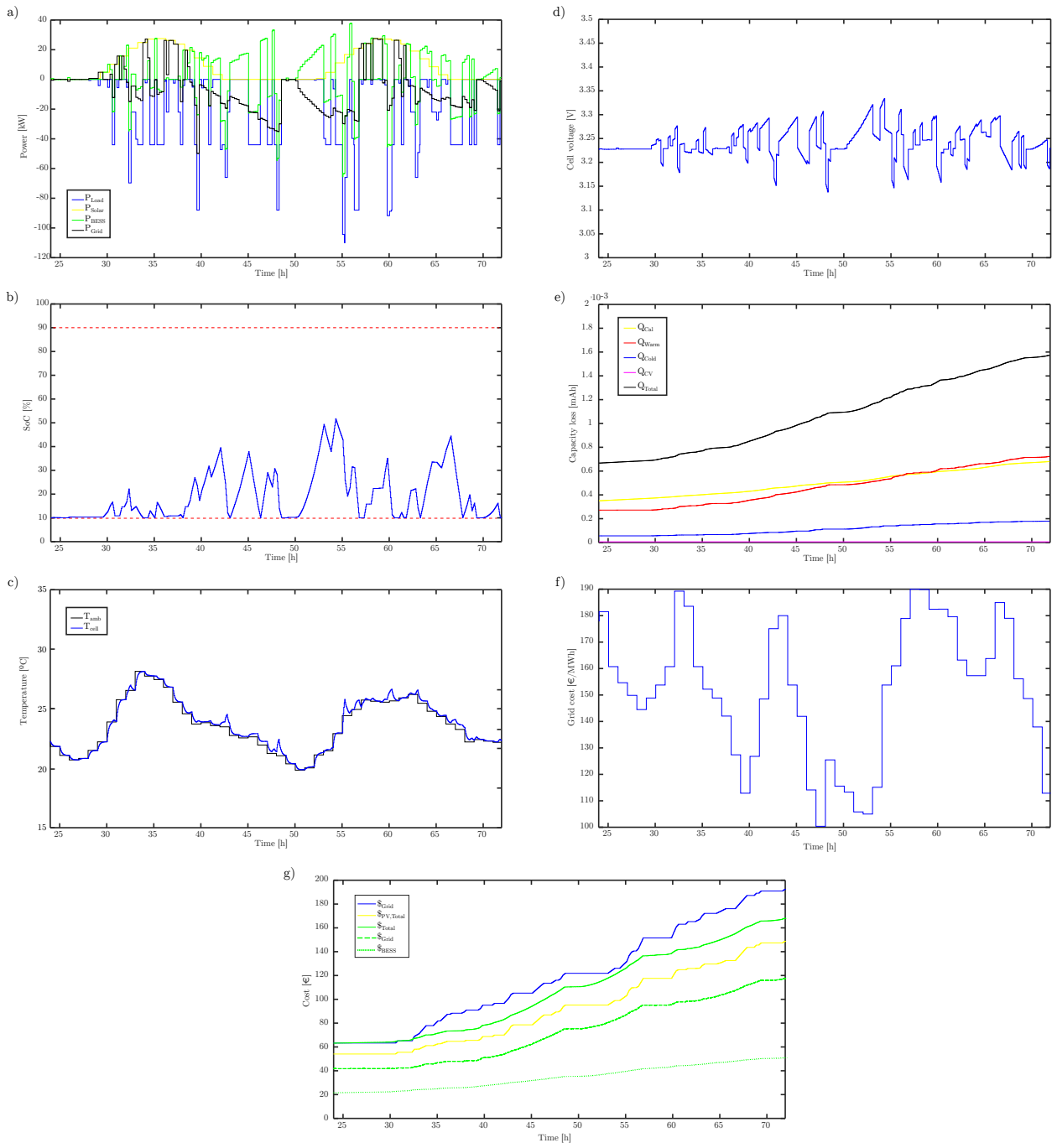

Fig. 3. Summertime results after two days operation (complete analysis correspond to one week), a) power profile b) SoC c) Cell temperature d) Cell voltage e) Cell capacity loss f) Grid cost g) System operation cost.

TABLE III
Results for summer and winter after one week opertaion.

Scenarios	Cost (€)			Capacity loss (mAh)					Grid power peak [kW]	Comply with Constraints
	Grid	Battery	Total	Calendar	Cold	Warm	CV	Total		
E1	488,78	-	488,78	-	-	-	-	-	132	-
E2w	449,93	-	449,93	-	-	-	-	-	132	-
E2s	379,63	-	379,63	-	-	-	-	-	132	-
E3w	418,46	97,09	515,55	0,957	0,829	1,55	0,01	3,346	53.47	Yes
E3s	309,02	94,81	403,83	1,392	1,523	0,353	0	3,268	49.83	Yes

22% during the summer. Including PV and BESS (E3) further reduces the grid costs by 14% (winter) and 36% (summer), but the overall total costs increase due to the battery depreciation. E2 was the most affordable among all the scenarios. However, there are other benefits for the E3 scenario, such as reduction in peak grid power, which were not economically quantified in this study and might offset some of the extra costs. Future research will investigate these opportunities.

VI. Conclusions

A nonlinear model predictive control framework was proposed for managing the energy of an EV charging station with onsite solar energy generation and battery storage. The control framework focused on reducing the economic operating costs related to the grid and the battery degradation, while enforcing temperature, voltage, charge and current limits. Simulation results demonstrated that our approach is able to reduce the grid costs in up to 36% (when compared to charging stations without battery and PV generation). It also reduced oscillations and peak grid power in 62.3%.Future work will focus on combined sizing and energy management of the EV charging station, improving tuning of the MPC cost function and experimental validation.

Acknowledgment

Authors would like to thank Dr Michael Schimpe from AUDI AG for sharing the battery model used in this work.

J.V.B. work is financed by the European Union - NextGenerationEU, as beneficiary of a Maria Zambrano International Talent Attraction Grant.

Appendix A

TABLE IV
Coefficients of the electrical resistance model.

Parameter	Value	Parameter	Value
a_{ch}	0,0656	a_{dch}	0,09
b_{ch}	-0,0362	b_{dch}	-0,0573
c_{ch}	0,02	c_{dch}	0,0309
d_{ch}	0,0021	d_{dch}	-0,0012

References

[1] European parliament, "energy policy - general principles" november 26, 2020. Accessed: April 26th, 2023. [Online]. Available: https://www.europarl.europa.eu/factsheets/en/sheet/68/energy-policy-general-principles

[2] California energy commission, "energy commission adopts standards requiring solar systems on new homes, first in nation," may 9, 2018. Accessed: April 26th, 2023. [Online]. Available: https://www.energy.ca.gov/news/2018-05/energy-commission-adopts-standards-requiring-solar-systems-new-homes-first

[3] "synthesis report 2022 on china's carbon neutrality: Electrification in china's carbon neutrality pathways." energy foundation china, beijing, china. Accessed: April 26th, 2023. [Online]. Available: https://www.efchina.org/Attachments/Report/report-lceg-20221104/Synthesis-Report-2022-on-Chinas-Carbon-Neutrality-Electrification-in-Chinas-Carbon-Neutrality-Pathways.pdf

[4] European commission (2020), 'sustainable and smart mobility strategy – putting european transport on track for the future'. Accessed: June 17th, 2023. [Online]. Available: https://eur-lex.europa.eu/legal-content/EN/TXT/?uri=CELEX\%3A52020SC0331

[5] S. Pareek, A. Sujil, S. Ratra, and R. Kumar, "Electric vehicle charging station challenges and opportunities: A future perspective," in 2020 International Conference on Emerging Trends in Communication, Control and Computing (ICONC3), 2020, pp. 1–6.

[6] F. J. G. Villalobos, "Optimized charging control method for plug-in electric vehicles in lv distribution networks," Ph.D. dissertation, Universidad del País Vasco= Euskal Herriko Unibertsitatea, 2016.

[7] R. Fachrizal, M. Shepero, D. van der Meer, J. Munkhammar, and J. Widén, "Smart charging of electric vehicles considering photovoltaic power production and electricity consumption: A review," eTransportation, vol. 4, p. 100056, 2020.

[8] H. H. Eldeeb, S. Faddel, and O. A. Mohammed, "Multi-objective optimization technique for the operation of grid tied pv powered ev charging station," Electric Power Systems Research, vol. 164, pp. 201–211, 2018.

[9] J. Zhang, Y. Zhang, T. Li, L. Jiang, K. Li, H. Yin, and C. Ma, "A hierarchical distributed energy management for multiple pv-based ev charging stations," in IECON 2018 - 44th Annual Conference of the IEEE Industrial Electronics Society, 2018, pp. 1603–1608.

[10] A. R. Bhatti and Z. Salam, "A rule-based energy management scheme for uninterrupted electric vehicles charging at constant price using photovoltaic-grid system," Renewable Energy, vol. 125, pp. 384–400, 2018.

[11] J. Sowe, J. Varela Barreras, M. Schimpe, B. Wu, C. Candelise, J. Nelson, and S. Few, "Model-informed battery current derating strategies: Simple methods to extend battery lifetime in islanded mini-grids," Journal of Energy Storage, vol. 51, p. 104524, 2022.

[12] M. Schimpe, J. V. Barreras, B. Wu, and G. J. Offer, "Battery degradation-aware current derating: An effective method to prolong lifetime and ease thermal management," Journal of The Electrochemical Society, vol. 168, no. 6, p. 060506, jun 2021.

[13] M. Schimpe, M. E. von Kuepach, M. Naumann, H. C. Hesse, K. Smith, and A. Jossen, "Comprehensive modeling of

temperature-dependent degradation mechanisms in lithium iron phosphate batteries," Journal of The Electrochemical Society, vol. 165, no. 2, p. A181, jan 2018.
[14] J. Martínez-Lao, F. G. Montoya, M. G. Montoya, and F. Manzano-Agugliaro, "Electric vehicles in spain: An overview of charging systems," Renewable and Sustainable Energy Reviews, vol. 77, pp. 970–983, 2017.
[15] N. Andrenacci, F. Karagulian, and A. Genovese, "Modelling charge profiles of electric vehicles based on charges data [version 3; peer review: 2 approved]," Open Research Europe, vol. 1, no. 156, 2022.
[16] Jrc photovoltaic geographical information system (pvgis) - european commission. Accessed: 08.05.2023. [Online]. Available: https://re.jrc.ec.europa.eu/pvg_tools/es/
[17] M. Schimpe, M. Naumann, N. Truong, H. C. Hesse, S. Santhanagopalan, A. Saxon, and A. Jossen, "Energy efficiency evaluation of a stationary lithium-ion battery container storage system via electro-thermal modeling and detailed component analysis," Applied Energy, vol. 210, pp. 211–229, 2018.
[18] Precios horarios del mercado diario en españa | omie. Accessed: April 26th, 2023. [Online]. Available: https://www.omie.es/es/file-access-list?parents%5B0%5D=/&parents%5B1%5D=Mercado%20Diario&parents%5B2%5D=1.%20Precios&dir=Precios%20horarios%20del%20mercado%20diario%20en%20Espa%C3%B1a&realdir=marginalpdbc
[19] F. Duffner, M. Wentker, M. Greenwood, and J. Leker, "Battery cost modeling: A review and directions for future research," Renewable and Sustainable Energy Reviews, vol. 127, p. 109872, 2020.
[20] J. Löfberg, "Yalmip : A toolbox for modeling and optimization in matlab," in In Proceedings of the CACSD Conference, Taipei, Taiwan, 2004.
[21] A. Wächter and L. T. Biegler, "On the implementation of an interior-point filter line-search algorithm for large-scale nonlinear programming," Mathematical programming, vol. 106, pp. 25–57, 2006.